

Search for Non-thermal Dark Matter through Monojet Signatures Associated with a Bottom Quark

Ucheol Jeon, Seulgi Kim, Jason S.H. Lee, Ian James Watson

University of Seoul

2025 NSRI Workshop
January 14, 2025



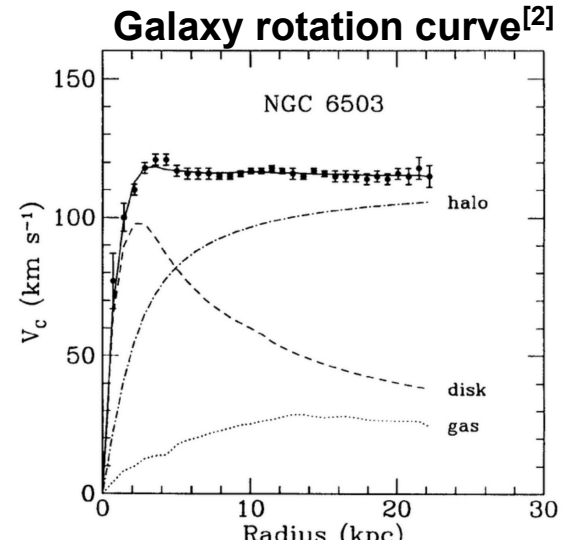
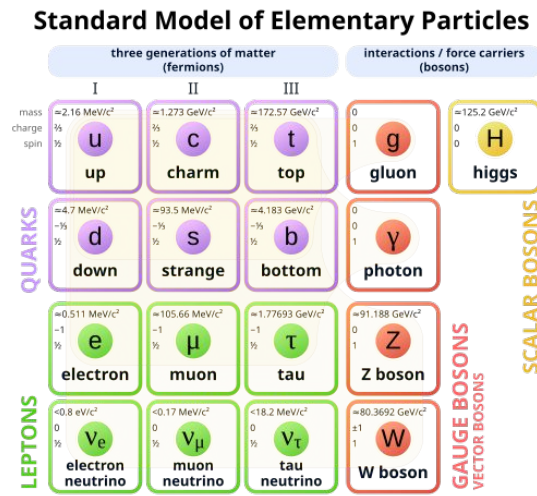
Introduction

The Standard Model

- Although the Standard Model (SM) is a successful theory describing fundamental particles, forces, and interactions, the SM has several limitations

Limitation of the Standard Model

- Baryon Asymmetry
 - Matter and Antimatter asymmetry
⇒ Theoretical prediction \neq Observation
 - Sakharov conditions**^[1] to explain the asymmetry
 - BSM models proposed with the condition
- Dark Matter
 - galaxy rotation curves ⇒ dark matter (DM)^[2]
 - various DM models have been proposed
WIMPs, Axions, Sterile neutrinos, ect



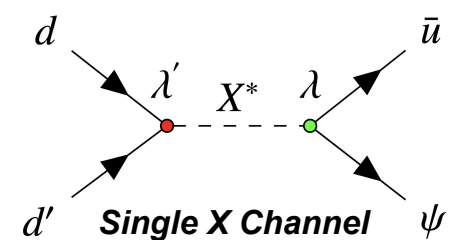
[1] A D Sakharov, Violation of CP in Variance, C Asymmetry, and Baryon Asymmetry of the Universe, 1991.

[2] T. S. van Albada, J. N. Bahcall, K. Begeman, and R. Sancisi, 'Distribution of Dark Matter in the Spiral Galaxy NGC 3198', *Astrophysical Journal*, 295 (1985), pp. 305–313, doi:10.1086/163375.

The Model Setup

Benchmark Model

- Interaction Lagrangian $\mathcal{L}_{int} \supset \lambda_{\alpha i} X_{\alpha} \psi u_i^c + \lambda'_{\alpha i j} X_{\alpha}^* d_i^c d_j^c + \frac{m_{\psi}}{2} \bar{\psi}^c \psi + \text{h.c.}$
 - X_{α} : Two iso-singlet color-triplet scalars ($\alpha = 1, 2$)
 - ψ : Majorana fermion (hypercharge 0) | DM candidate
 - $X_{\alpha}^* d_i^c d_j^c$: Quark fusion interaction
 - $X_{\alpha} \psi u_i^c$: Interaction with up-type quark and DM candidate
 - $\lambda'_{\alpha i j}$, $\lambda_{\alpha i}$: coupling constant i, j flavour indices $i \neq j$



Monojet Signature

- Final state of monojet signature
 - One **b quark**, one **light quark**, and large **MET** from ψ
- Monojet signature

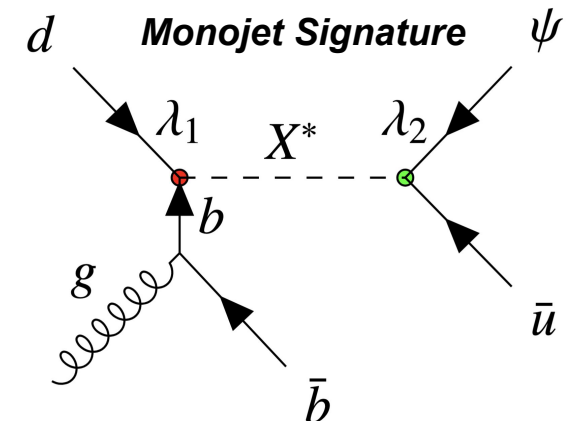
$$\mathcal{L}_{int} \supset \lambda_{\alpha i} X_{\alpha} \psi u_i^c + \lambda'_{\alpha i j} X_{\alpha}^* d_i^c d_j^c + \frac{m_{\psi}}{2} \bar{\psi}^c \psi + \text{h.c.}$$

Coupling Condition

Allow : coupling of X to **u quark only**
The fusion of **d-b** and **s-b quarks**

$$\mathcal{L}_{monojet} \supset \lambda_{\psi u} X_1 \psi u^c + \lambda_{db} X_1^* d^c b^c + \lambda_{sb} X_1^* s^c b^c + \text{h.c.}$$

λ_2 λ_1



LHC and CMS

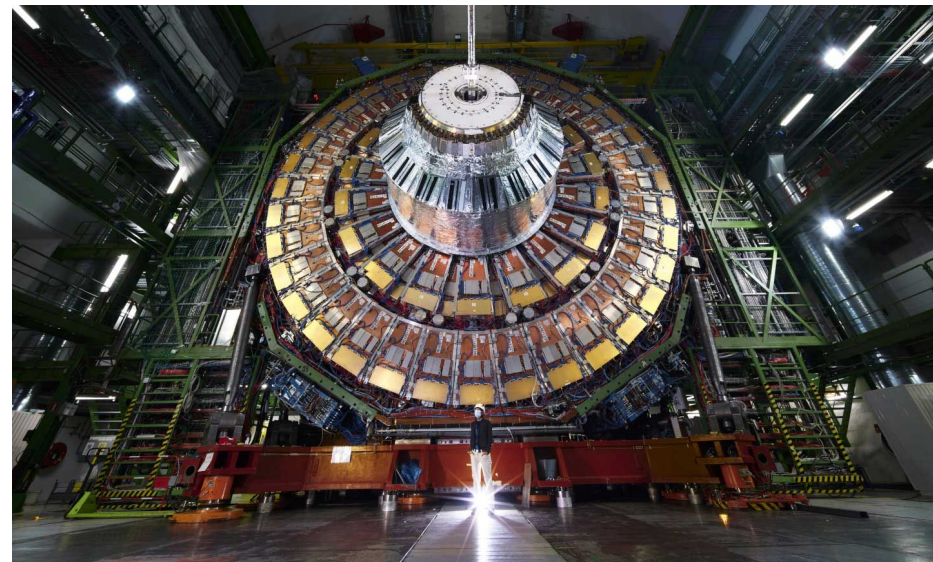
Large Hadron Collider (LHC)

“The world's largest and highest-energy particle accelerator”



Compact Muon Solenoid (CMS)

“one of two large general-purpose particle physics detectors built on LHC”



Simulation

Monte-Carlo Simulation Sample Production

- MadGraph5_aMC@NLO (v2.6.7) for **pp collisions at $\sqrt{s} = 13$ TeV**
Parton showering and hadronization : PYTHIA8 (v8.244)
Detector simulation : DELPHES (v3.4.2) Modified **CMS-like detector configuration**
- Signal Modeling and Coupling Grid
 - The $m_{X_1} = 1.0, 1.5, \text{ and } 2.0$ TeV with $m_{X_2} = 10$ TeV and $m_\psi = 1$ GeV
 - On a 2-dim coupling grid (15, 14) :
 $\lambda_1 = \{0.03, 0.05, \dots, 1.0\}$, $\lambda_2 = \{0.04, 0.06, \dots, 1.0\}$
- Backgrounds information
 - Generated background processes:
 $W+jets$ (WJ), $Z+jets$ (DY), $TTbar$ (TT), and Di-boson(VV)
 - WJ , DY , and TT
⇒ Generated with up to three additional ISR/FSR jets

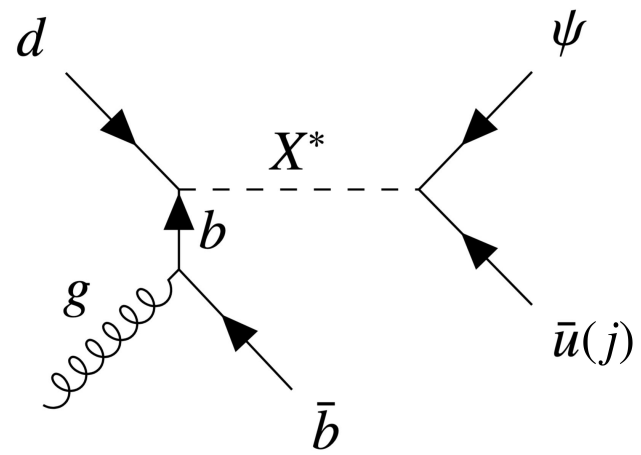
λ_1	cross section σ [fb]			
	λ_2			
	0.1	0.2	0.5	1.0
0.1	11.69	28.22	46.46	51.00
0.2	12.83	43.22	130.87	182.48
0.5	13.04	50.91	268.25	683.89
1.0	14.24	56.88	340.55	1159.29

Several cross-section for production of X_1 with 1.0 TeV mass point

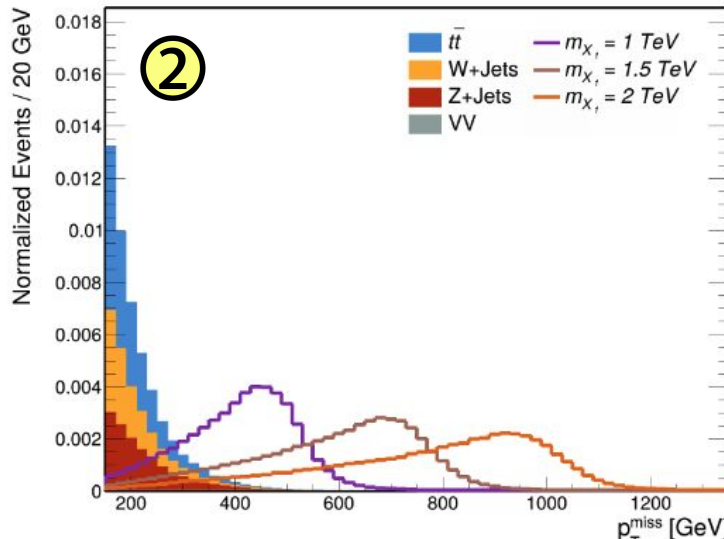
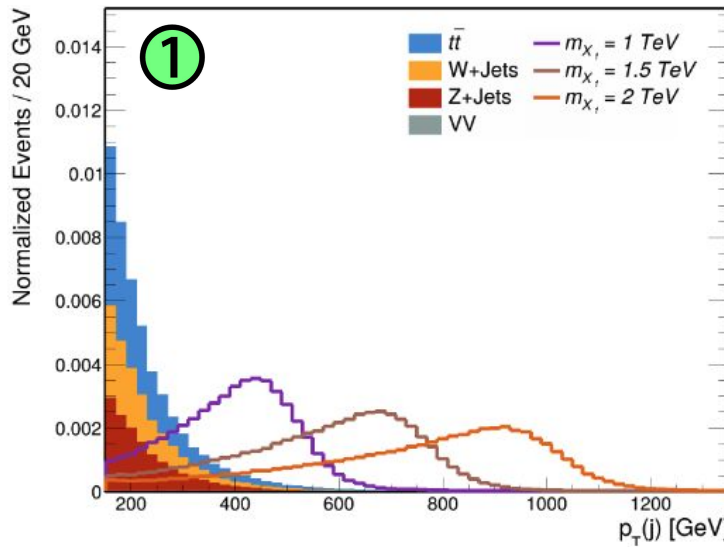
Analysis

Object and Event Selections

- Signal topology (Remind)
 - One **b**-tagged jet (**b**)
 - One **light quark jet (j)** and
 - Large **transverse missing energy (ψ)**
↔ DM candidate
- Selection description
 - One b-tagged jet selection :
 $p_T(b) > 20 \text{ GeV}$ $|\eta(b)| < 2.4$
 - One light quark jet selection :
 $p_T(j) > 150 \text{ GeV}$ $|\eta(j)| < 2.4$
 - Missing Transverse Energy :
 $p_T^{\text{miss}} > 150 \text{ GeV}$
 - Lepton (e/μ) and τ tagged jet event veto :
 $p_T > 10 \text{ GeV}$ $|\eta| < 2.4$
applied to suppress backgrounds from $W(\rightarrow \ell\nu) + \text{jets}$ and $t\bar{t}$ with leptonic decays

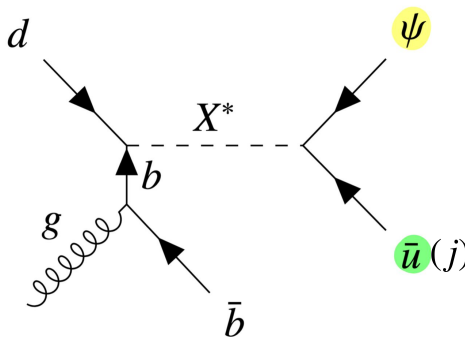


Analysis

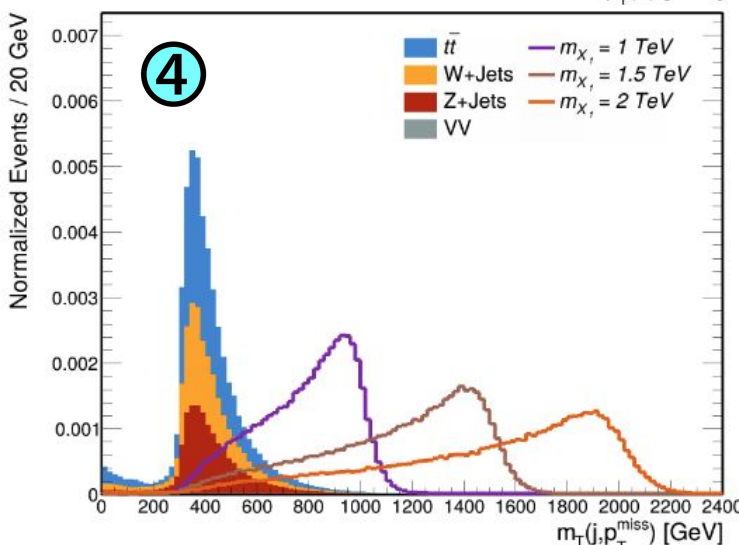
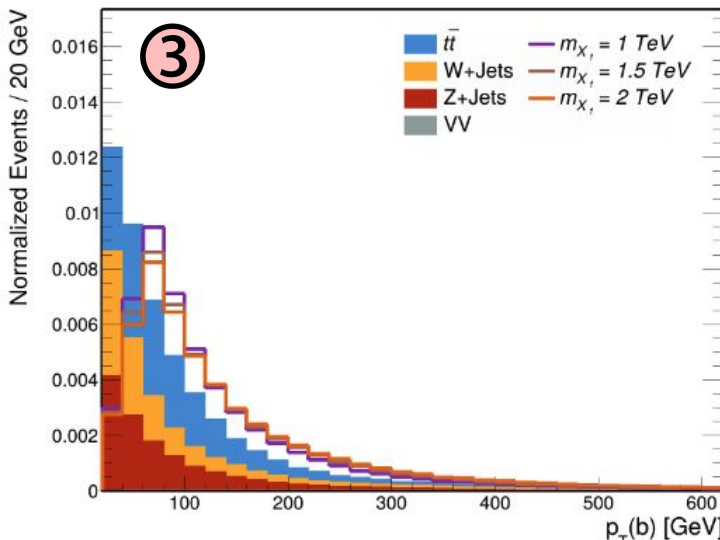


Kinematic distributions

- Objects from mediator X
 - The light jet
 - p_T^{miss} : transverse missing momentum
⇒ Both carry much higher p_T than background
- Characteristic features
 - For each m_{X_1} both leading jet p_T and p_T^{miss}
⇒ Jacobian-like peak near $p_T \sim m_{X_1}/2$
⇒ due to two-body decay kinematics of X

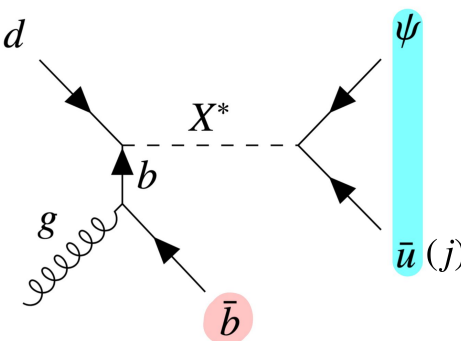


Analysis



Kinematic distributions

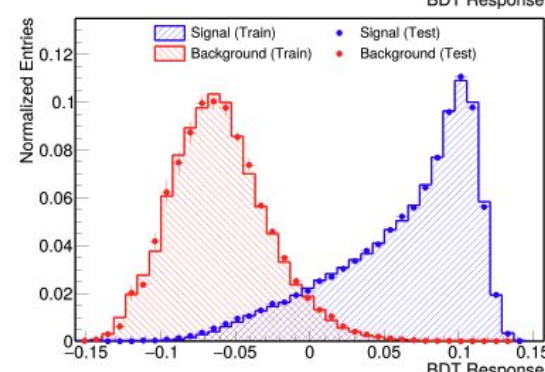
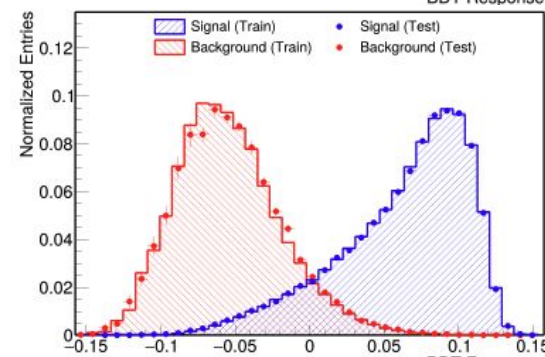
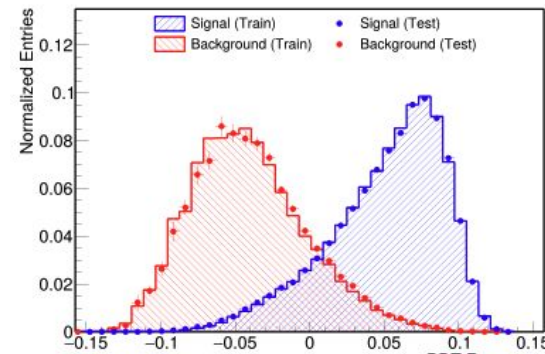
- Gluon splitting
 - The b-tagged jet arises from gluon splitting
⇒ soft b-jet concentrated at low p_T
- Transverse mass distribution
 - $m_T(j, p_T^{\text{miss}})$ shows endpoint close to m_{X_1}
 - Signal produces harder m_T spectrum than background
 - As m_{X_1} increases, endpoint shifts to higher values



Analysis

BDT Training and Performance

- Boosted Decision Tree (BDT)
 - Machine-learning–based classifier trained
⇒ Lead to enhanced **signal–background discrimination**
- Training setup
 - Separate BDT model trained for each X_1 mass point
 - Signal : all combinations of $(\lambda_1, \lambda_2) \in \{0.1, 0.3, 1.0\}^2$
 - Background : all main background processes
- Input variables (total 10)
 - $p_T(j)$, $p_T(b)$, $\underline{p_T^{\text{miss}}}$
 - $\eta(j)$, $\eta(b)$
 - $\Delta\phi(j, b)$, $\Delta\phi(b, p_T^{\text{miss}})$, $\Delta\phi(p_T^{\text{miss}}, j)$
 - $\Delta R(j, b)$, $m_T(p_T^{\text{miss}}, j)$



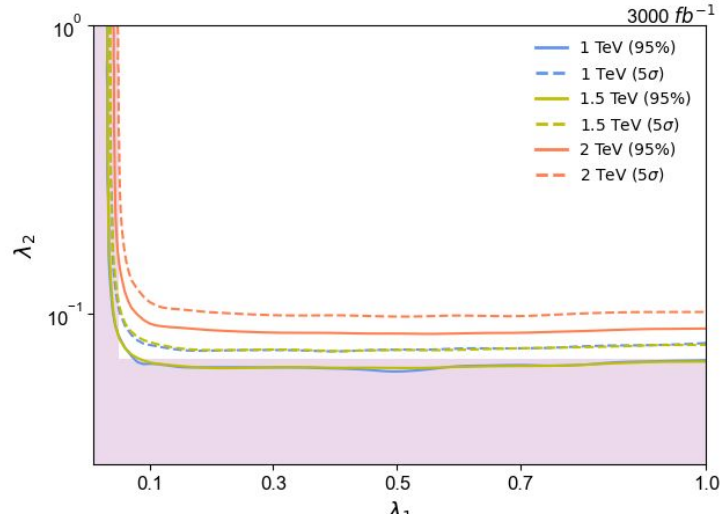
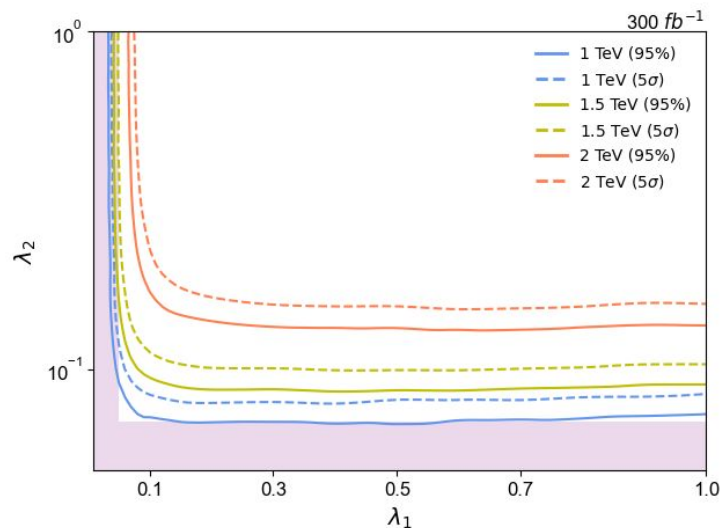
Results

- **Statistical evaluation : Bayesian approach**
- MC Statistics : 1.84 - 3.64 %
 - Systematic error has become important
→ *Working in Progress*
- **95 % Confidence Level Exclusion Limit and 5 σ Discovery Potential Line**
- Exclusion region (95% CL)

Run 3 300 fb^{-1}	m_{X_1} [TeV]		
	1.0	1.5	2.0
λ_1	> 0.03	> 0.04	> 0.06
λ_2	> 0.07	> 0.09	> 0.13

HL-LHC 3000 fb^{-1}	m_{X_1} [TeV]		
	1.0	1.5	2.0
λ_1	> 0.03	> 0.03	> 0.04
λ_2	> 0.06	> 0.06	> 0.09

- If the coupling goes beyond **this limit**, the signal is excluded at 95% CL
- Higher m_{X_1} → exclusion sensitivity decreased
- Higher luminosity → stronger exclusion limits due to more signal events
- **Purple solid area** ⇒ hadronization region



Results; Comparison with CMS analysis^[7]

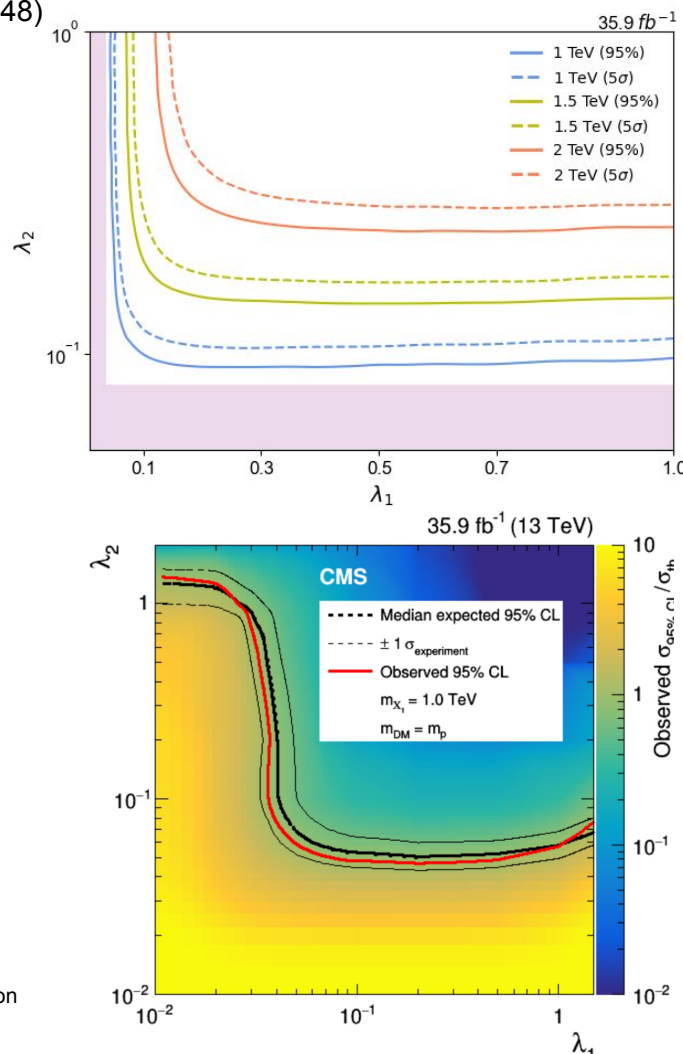
- CMS collaboration performed a monojet analysis(CMS-EXO-16-048)
- In that study, b-tagged jets were vetoed
⇒ **This study is comparably** (associated with a b quark)
- 35.9 fb^{-1} of data collected at $\sqrt{s} = 13 \text{ TeV}$ (2016 Run)

- Exclusion region (95% CL) **2016 Run (35.9 fb^{-1})**

monojet	m_{X_1} [TeV]
	1.0
λ_1	> 0.04
λ_2	> 0.09

CMS Monojet Analysis	m_{X_1} [TeV]
	1.0
λ_1	> 0.04 (0.03)
λ_2	> 0.05 (0.05)

- The solid line in the CMS plot
⇒ the upper limit from the previous monojet analysis
- The exclusion region for λ_1 is shown as similar level



[3] C. M. S. Collaboration, 'Search for New Physics in Final States with an Energetic Jet or a Hadronically Decaying W or Z Boson and Transverse Momentum Imbalance at $\sqrt{s} = 13 \text{ TeV}$ ', Physical Review D, 97.9 (2018), p. 092005, doi:10.1103/PhysRevD.97.092005.

Summary

- We presented a study on **the search potential for a baryon-number-violating dark matter (DM) candidate** using a **b-associated monojet channel** involving a bottom jet, light-quark jet, and DM candidates.
- To complement previous monojet, our analysis introduces an additional b-tagged jet in the final state, improving the sensitivity to this specific interaction topology.
- The results are shown in the parameter space with **95% CL exclusion limits** and **5 σ discovery potential lines**, highlighting the experimental reach for given coupling and mass configurations.
- Compared to existing monojet analyses and b-associated monotop channel, this study provides **comparable coverage of the parameter space**.

Backup Slides

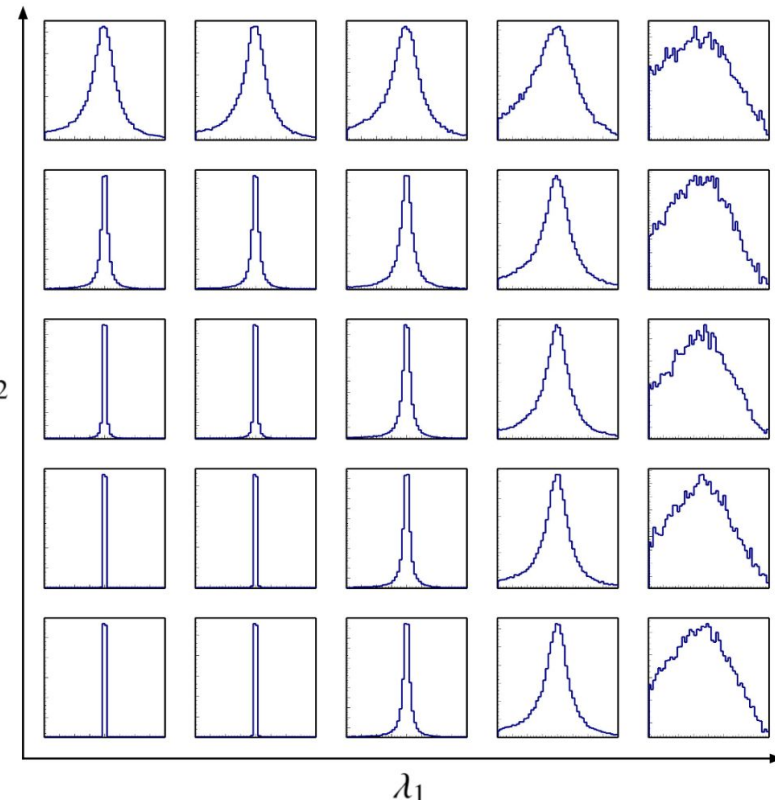
Simulation

Mass Distribution

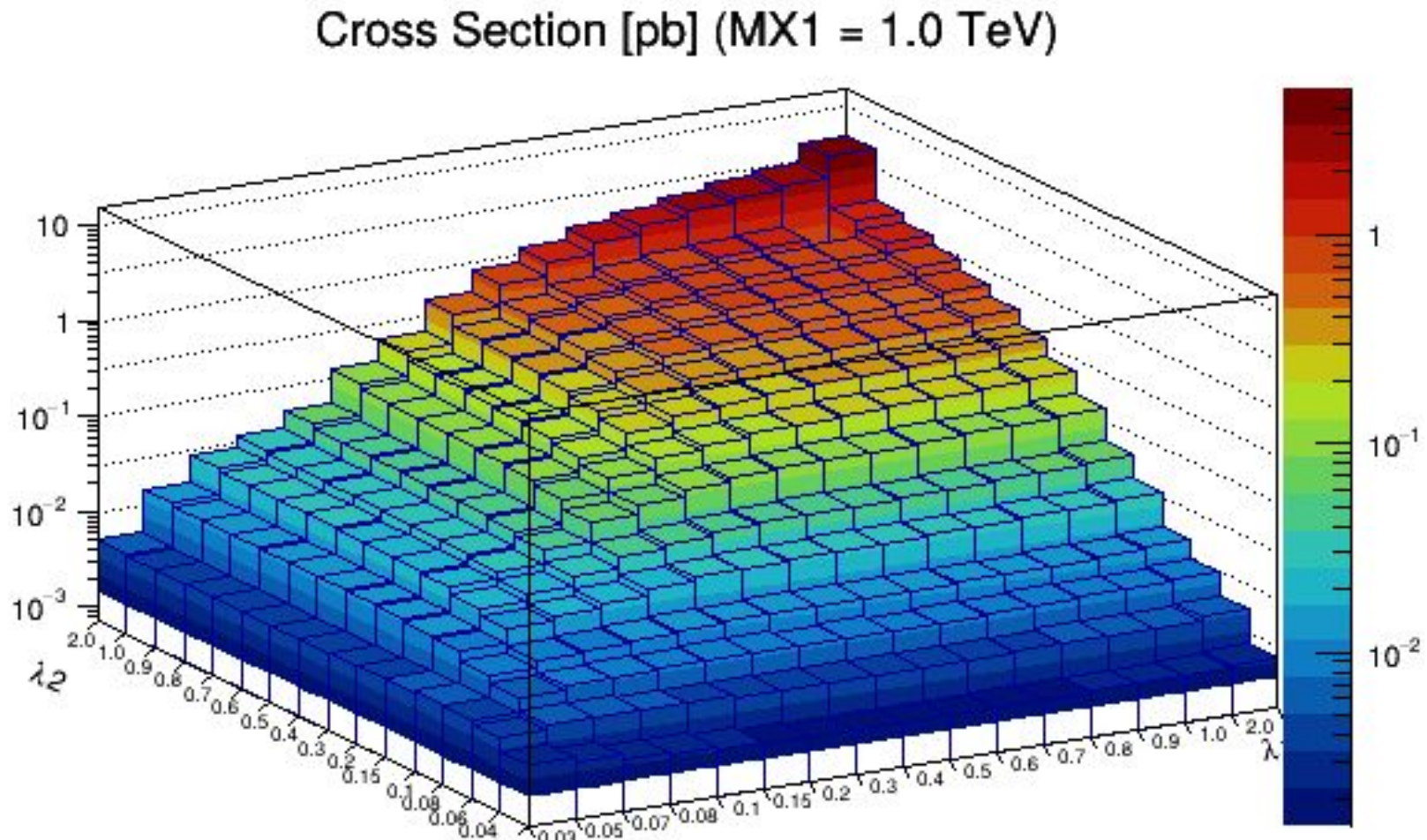
Generator level mass of x_1 distributions for 1.0 TeV sample with several (λ_1, λ_2) values :
 $\{0.08, 0.1, 0.5, 1.0, 2.0\}$.

Each plot shows the x-axis range of 800–1200 GeV divided into 50 bins, while the y-axis represents the normalized event yield. λ_2

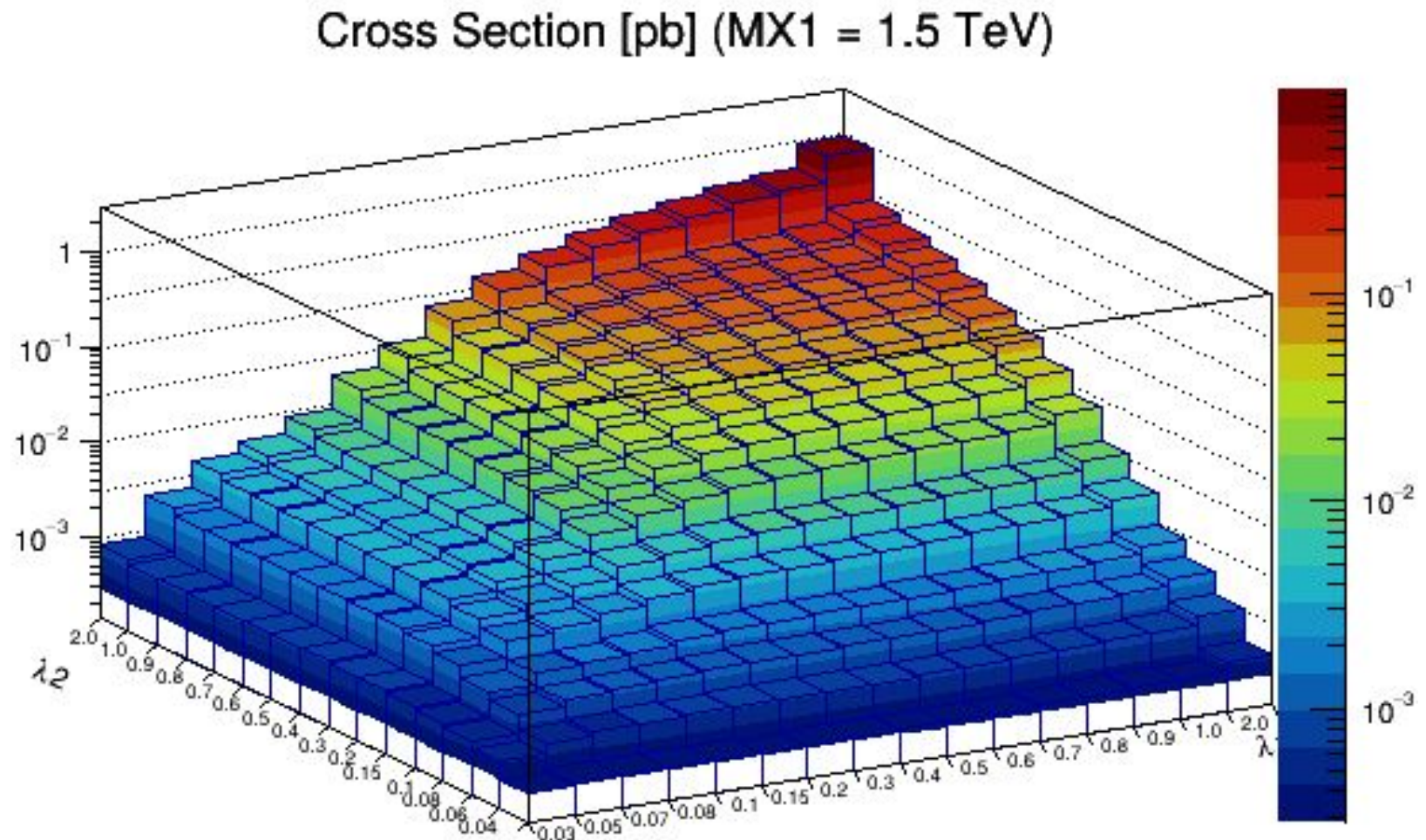
The case of $(\lambda_1 = 2.0)$, It appears to show different kinematics from others.



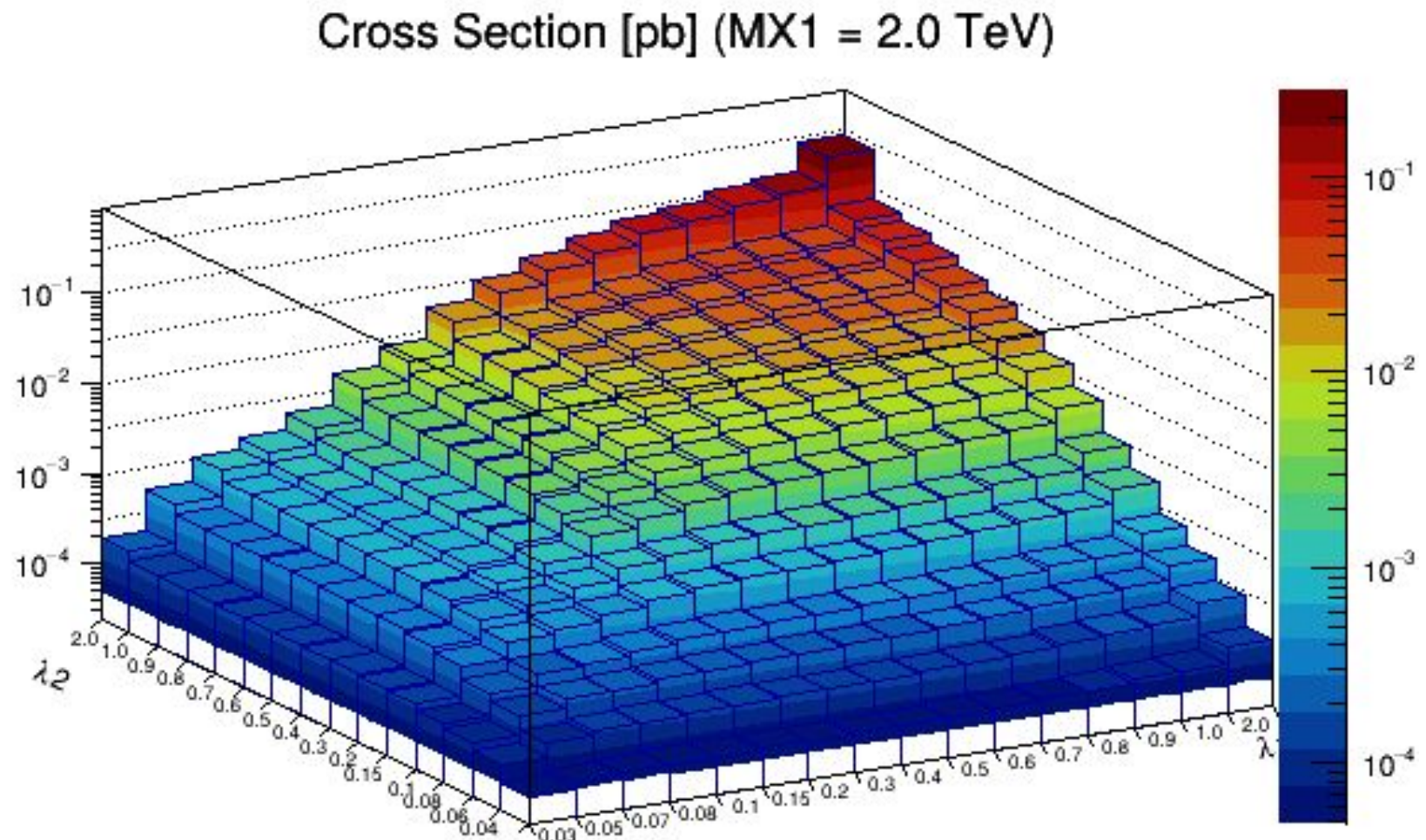
Cross-section 2D plot; 1.0 TeV signal



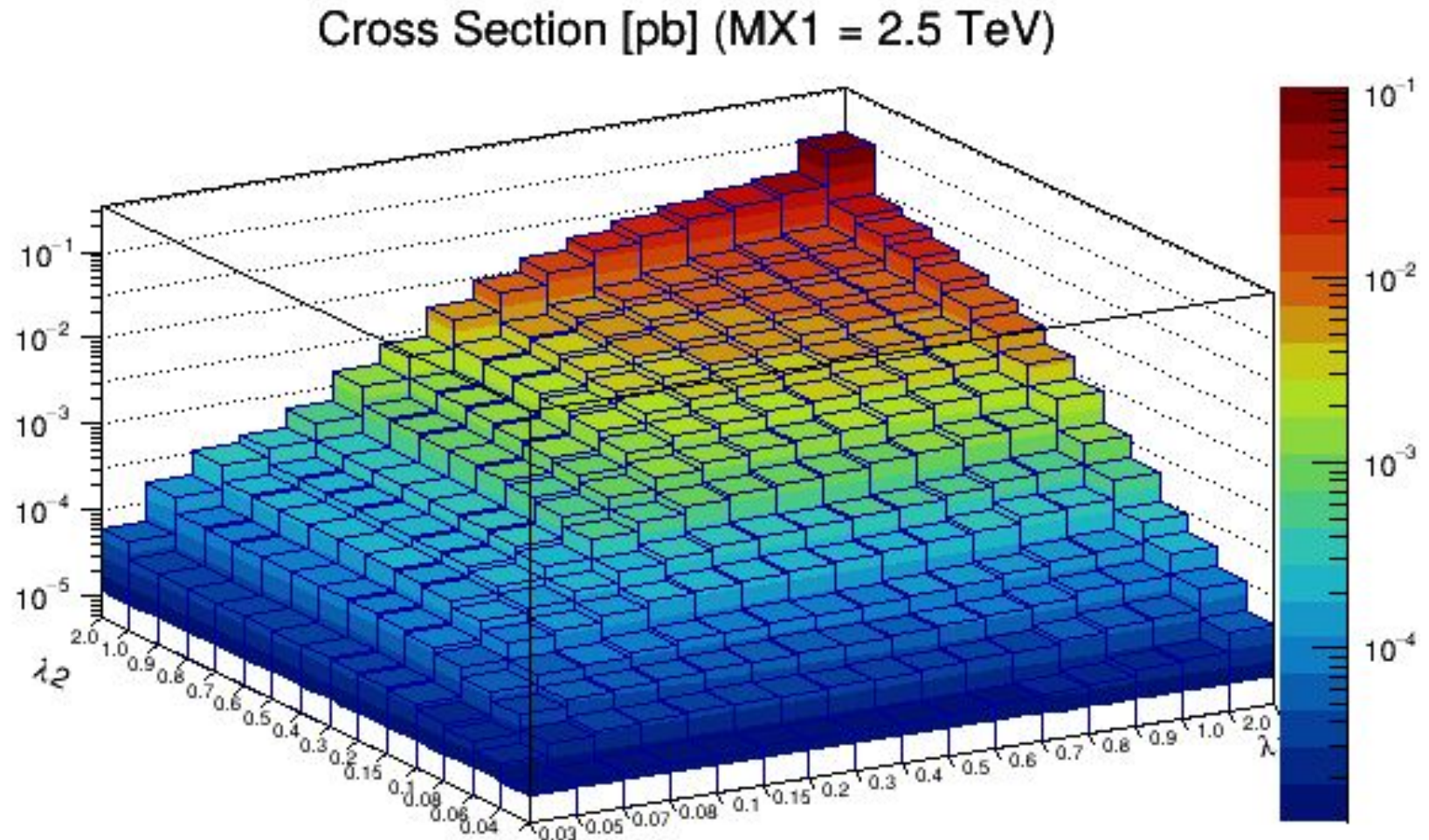
Cross-section 2D plot; 1.5 TeV signal



Cross-section 2D plot; 2.0 TeV signal



Cross-section 2D plot; 2.5 TeV signal



of events after selection

Backgrounds

Run3 Lumi	TT	DY	WJ	ZZ	Total
generated	165,137,700.0	67,059,895.4	305,904,769.0	13,173,705.8	551,276,070.0
l veto	97,875,346.6	65,331,800.8	148,834,524.0	6,394,586.6	318,436,259.0
ujet	12,627,962.2	10,842,621.0	20,479,855.5	165,958.8	44,116,397.5
bjet	5,927,747.5	662,997.1	1,250,993.0	21,757.3	7,863,495.0
met	351,373.9	236,314.1	225,546.8	2,657.9	815,892.7
Sel / Gen [%]	0.21%	0.35%	0.07%	0.02%	0.15%

Signals

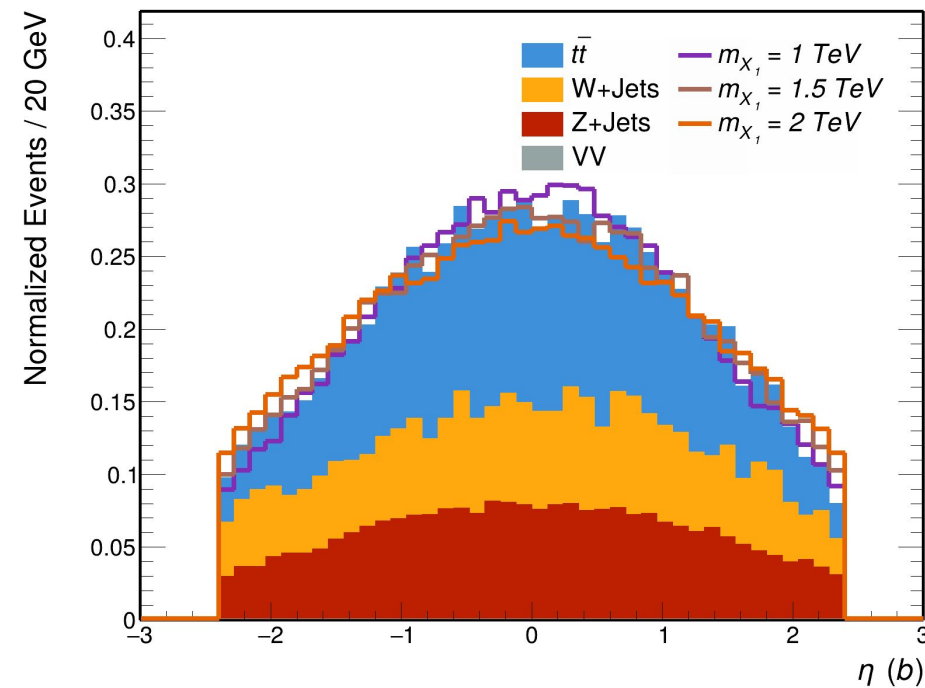
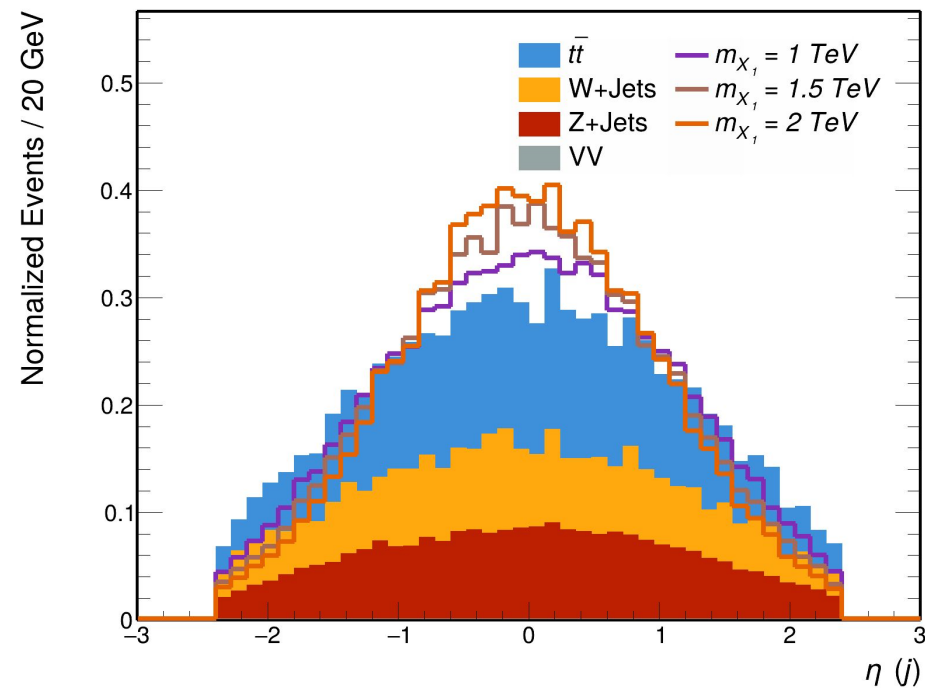
Run3 Lumi	1.0 (0.5, 0.5)	1.5 (0.5, 0.5)	2.0 (0.5, 0.5)
generated	80,475.3	11,979.9	2,549.0
l veto	75,684.1	11,242.1	2,387.8
ujet	51,881.2	7,313.4	1,465.5
bjet	30,598.9	4,288.3	849.2
met	29,620.6	4,230.4	842.6
Sel / Gen [%]	36.81%	35.31%	33.06%

Distribution

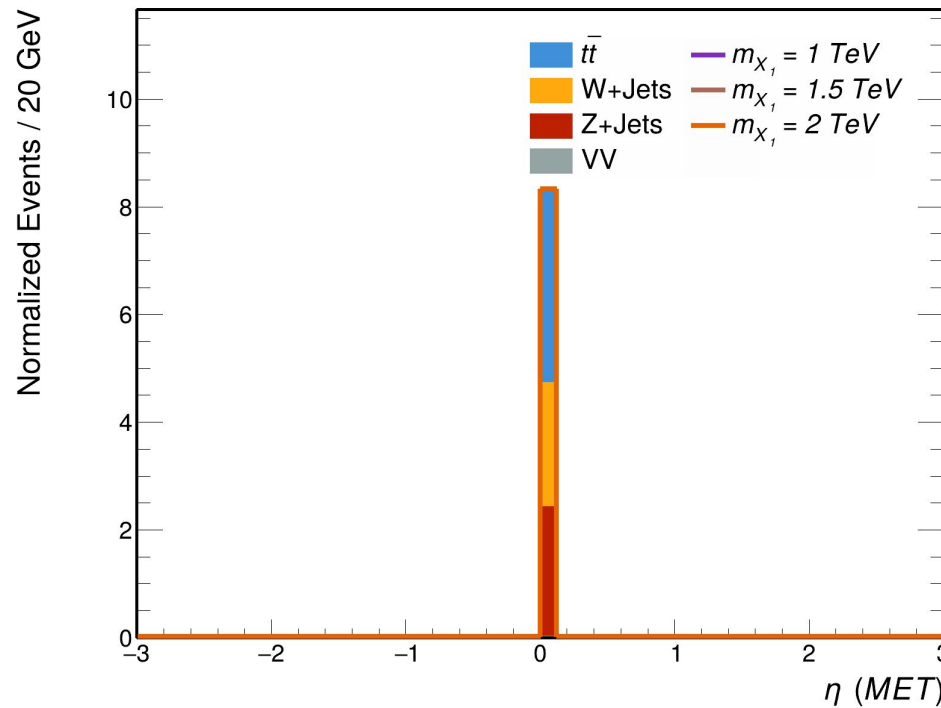
300 fb^{-1} (13 TeV)

- **Pseudorapidity (Eta or η) distribution**

- η distribution of j on left plot in $x \in [-3, 3]$
- η distribution of b on right plot in $x \in [-3, 3]$



- **Pseudorapidity (Eta or η) distribution**
 - η distribution of MET in $x \in [-3, 3]$ with normalized events
 - It's trivial result because η of MET is zero by definition

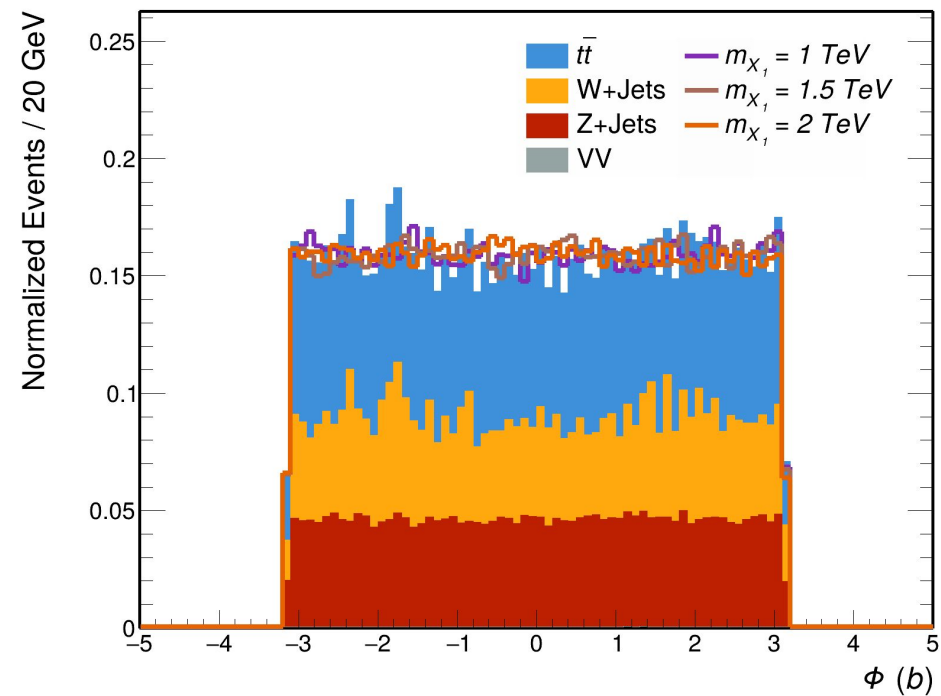
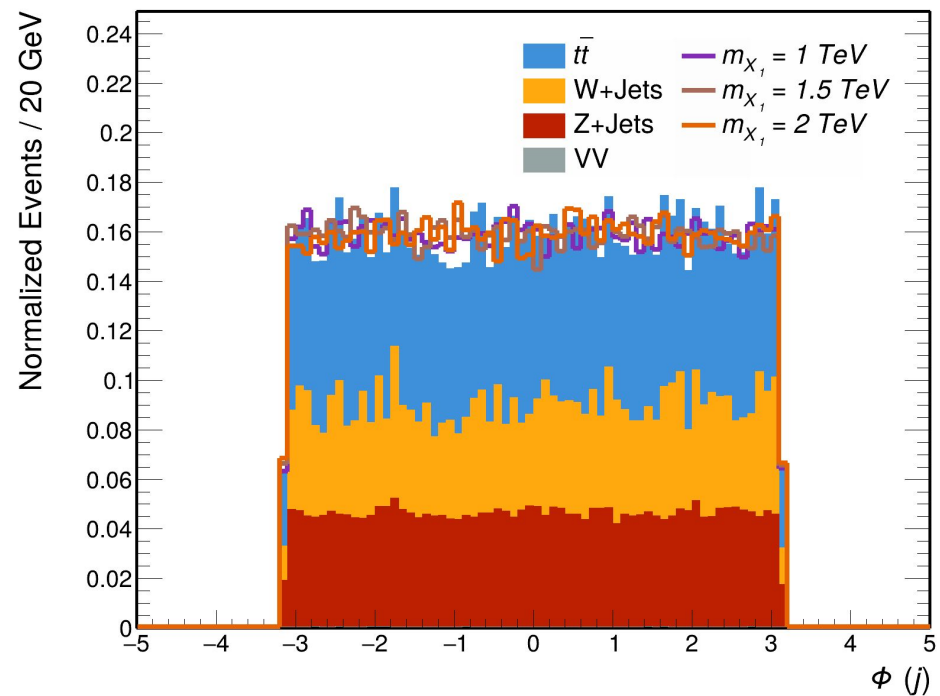


Distribution

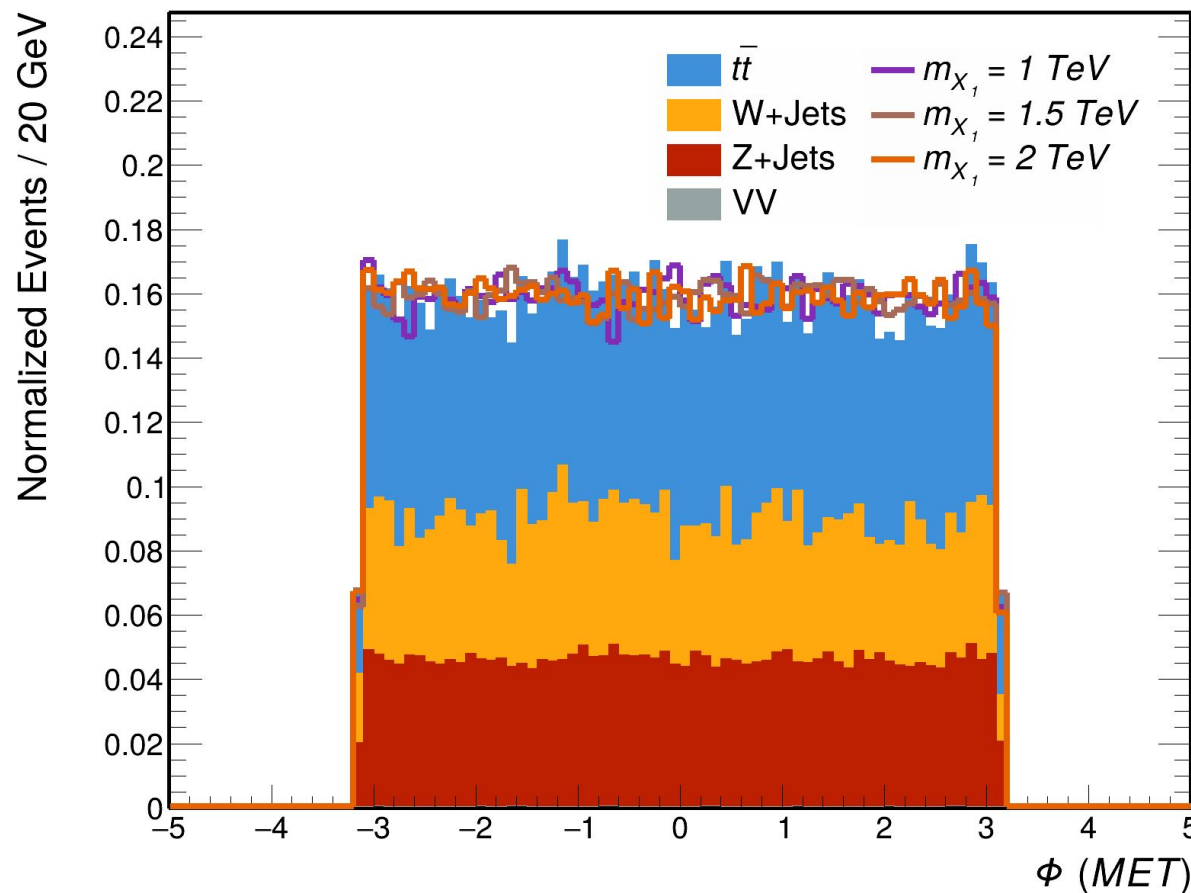
300 fb^{-1} (13 TeV)

- azimuthal angle (Phi or ϕ) distribution

- ϕ distribution of j on left plot in $x \in [-5, 5]$ with normalized events
- ϕ distribution of b on right plot in $x \in [-5, 5]$ with normalized events



- azimuthal angle (Phi or ϕ) distribution
 - ϕ distribution of MET in $x \in [-5, 5]$ with normalized events

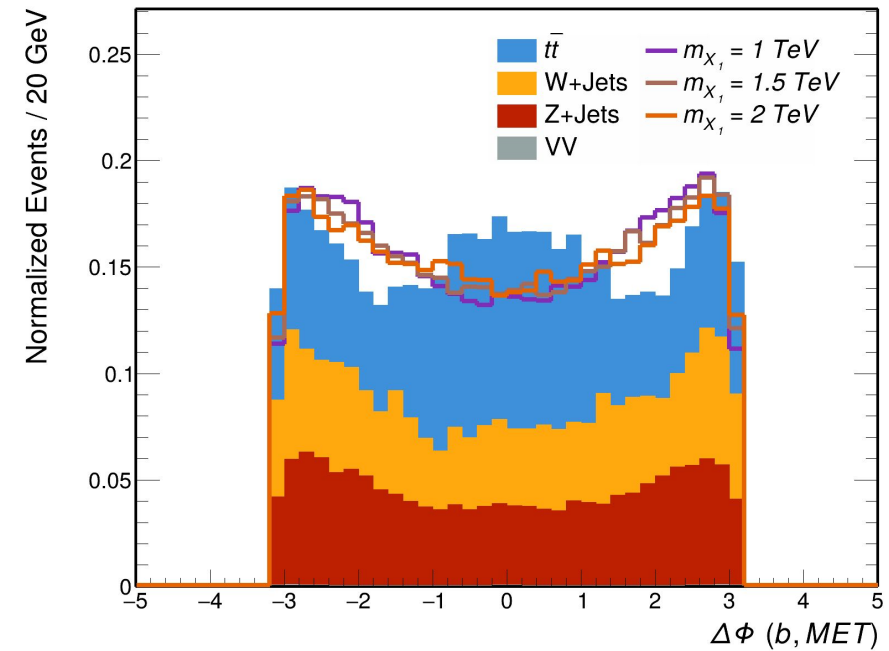
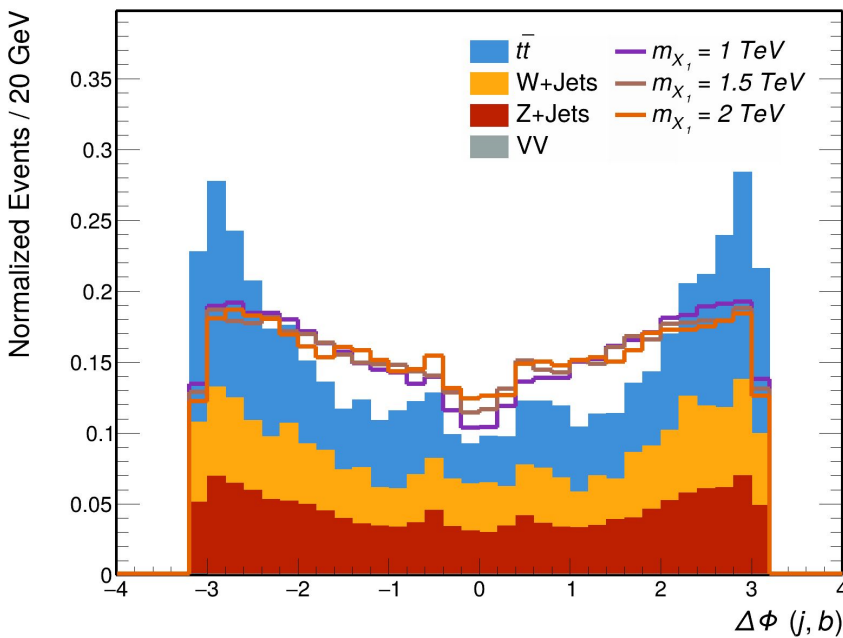


Distribution

300 fb^{-1} (13 TeV)

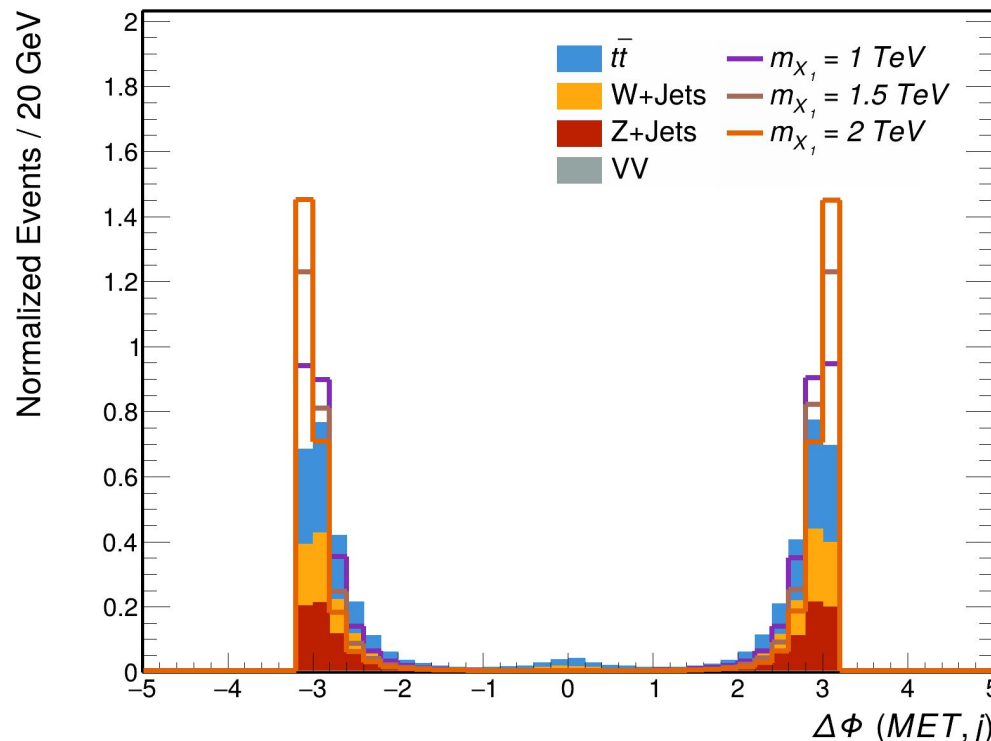
- **Azimuthal angle ($\Delta\phi$) distribution**

- $\Delta\phi$ distribution between j and b on left plot in $x \in [-4, 4]$ with Normalized events per bin
- $\Delta\phi$ distribution between b and MET on right plot in $x \in [-4, 4]$ with Normalized events per bin
- Definition : $\Delta\phi = \arctan2(\sin(\phi_i - \phi_j), \cos(\phi_i - \phi_j))$



- **Azimuthal angle ($\Delta\phi$) distribution**

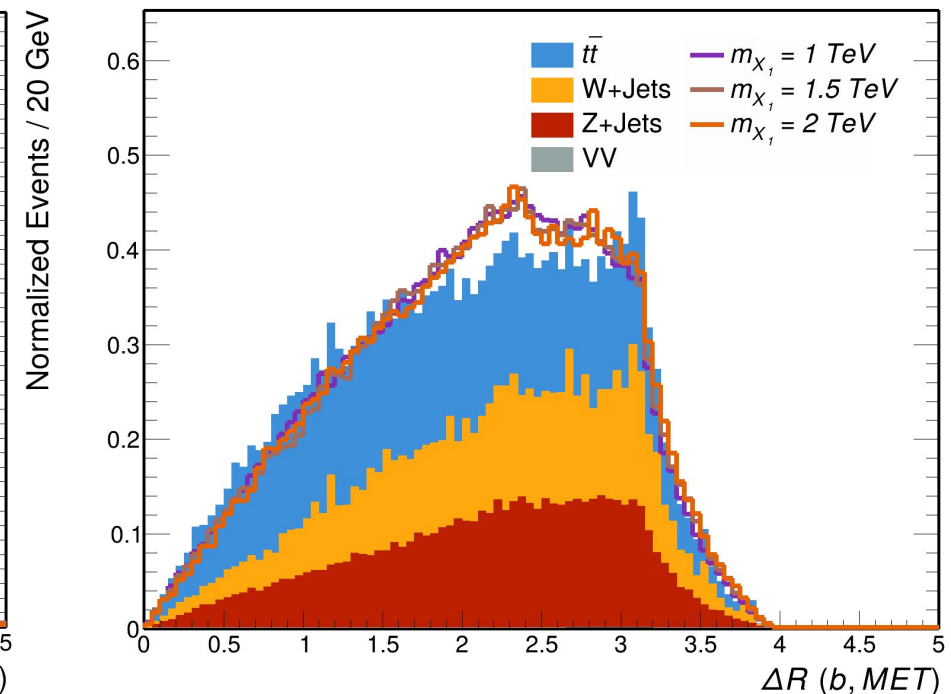
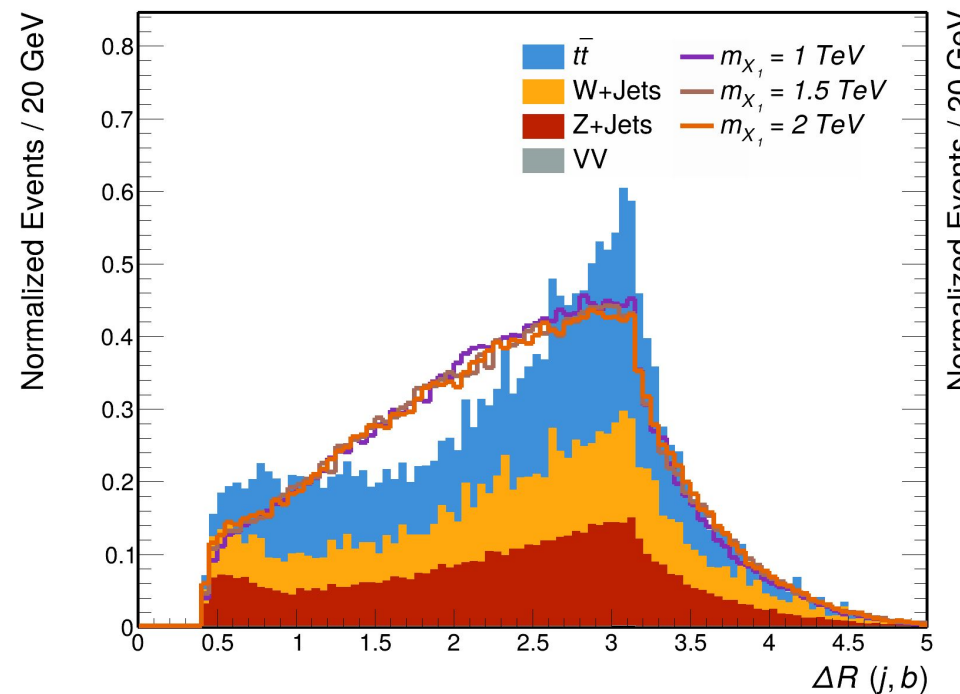
- $\Delta\phi$ distribution between MET and j on the plot in $x \in [-4, 4]$ with Normalized events per bin
- Definition : $\Delta\phi = \arctan2(\sin(\phi_i - \phi_j), \cos(\phi_i - \phi_j))$



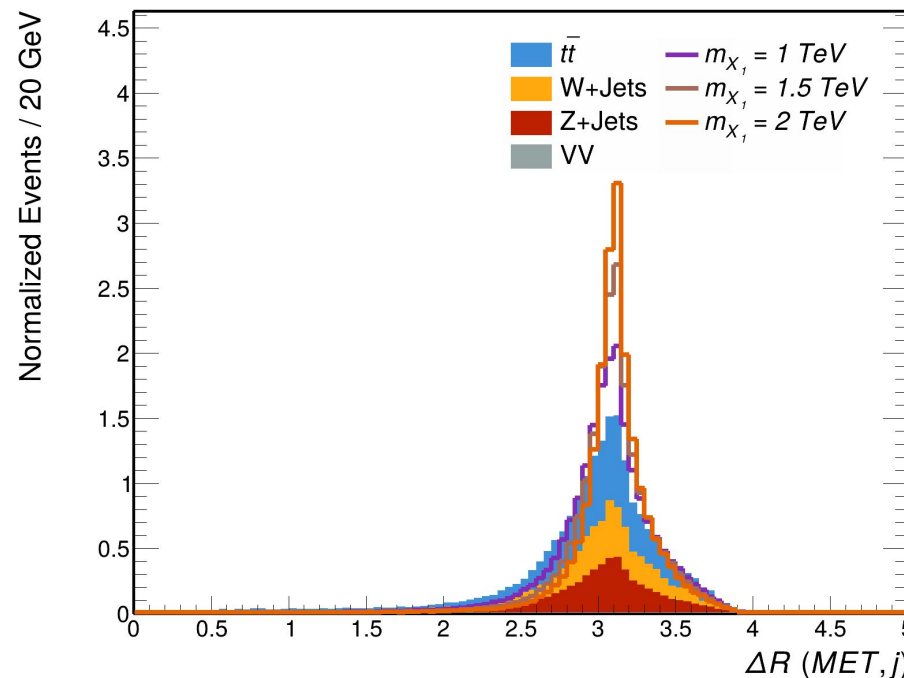
Distribution

300 fb^{-1} (13 TeV)

- **Distance between two objects in the detector's η - ϕ angle plane (ΔR)**
 - ΔR distribution between j and b on left plot in $x \in [0, 5]$ with Normalized events
 - ΔR distribution between b and MET on left plot in $x \in [0, 5]$ with Normalized events
 - Definition : $\Delta R = \sqrt{(\Delta\eta)^2 + (\Delta\phi)^2}$
Where $\Delta\phi = \text{arctan2}(\sin(\phi_i - \phi_j), \cos(\phi_i - \phi_j))$
 $\Delta\eta = \eta_i - \eta_j$



- **Distance between two objects in the detector's η - ϕ angle plane (ΔR)**
 - ΔR distribution between MET and j on left plot in $x \in [0, 5]$ with Normalized events
 - Definition : $\Delta R = \sqrt{(\Delta\eta)^2 + (\Delta\phi)^2}$
 where $\Delta\phi = \text{arctan2}(\sin(\phi_i - \phi_j), \cos(\phi_i - \phi_j))$
 $\Delta\eta = \eta_i - \eta_j$

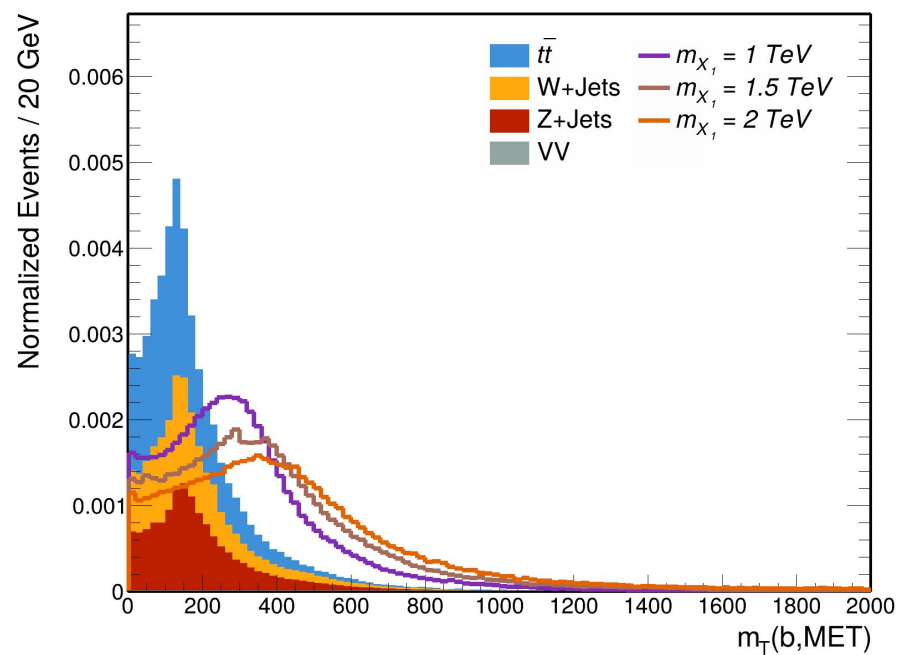
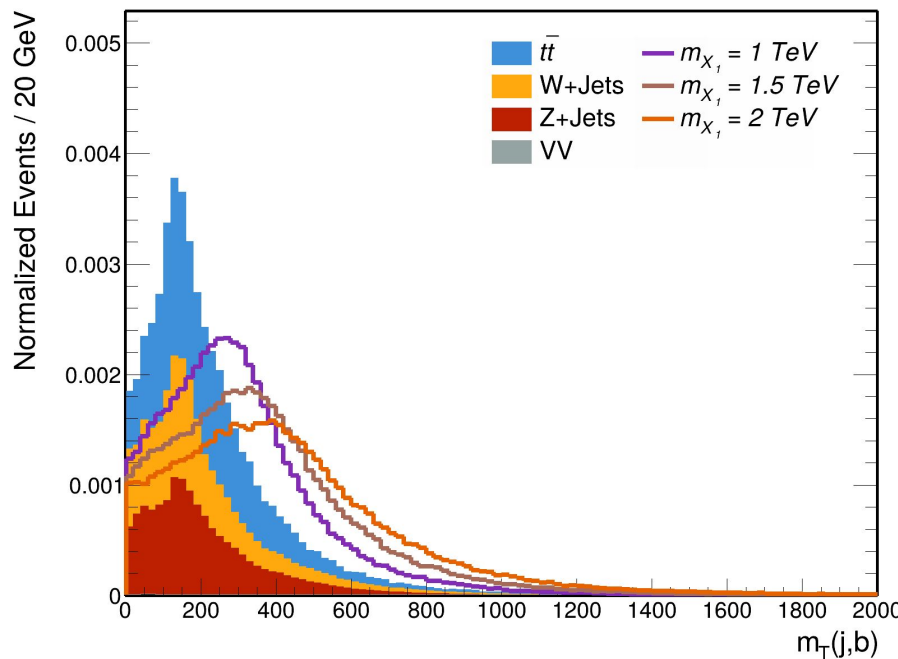


Distribution

300 fb^{-1} (13 TeV)

- **Transverse mass (M_T) distribution in two particle**

- M_T distribution between j and b on left plot in $x \in [0, 2000]$ with Normalized events per bin (20 GeV)
- M_T distribution between b and MET on right plot in $x \in [0, 2000]$ with Normalized events per bin (20 GeV)
- Definition : $M_T(i, j) = \sqrt{2 p_{T_i} p_{T_j} (1 - \cos \Delta\phi)}$



BDT Method

Boosted Decision Tree (BDT) Method

To determine appropriate candidate BDT cut values, significance is defined to: $S/\sqrt{S+B}$. On the top plot: The distribution of signal (S) It can be observed that the maximum significance is attained at a specific BDT value.

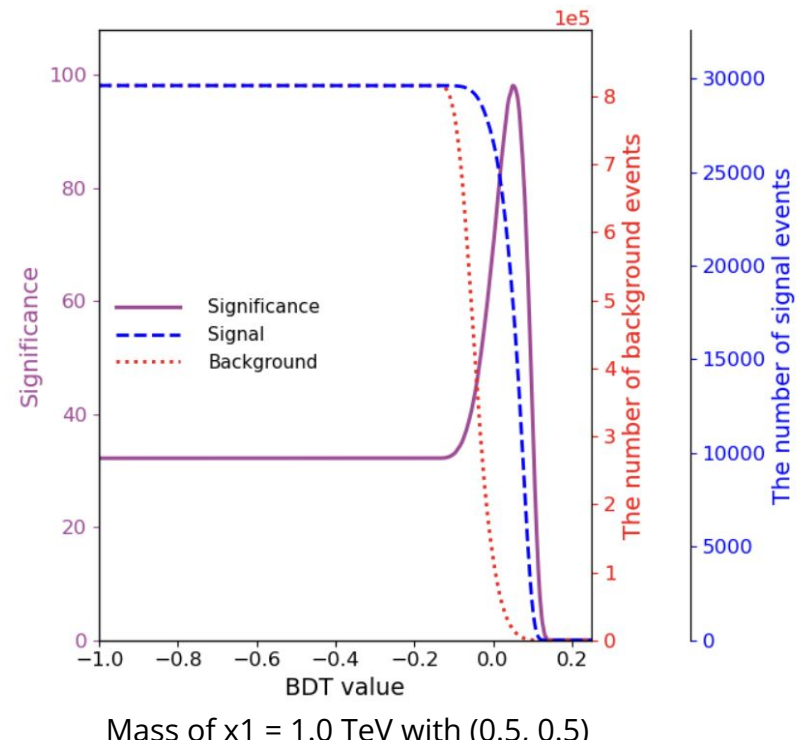
Furthermore, the AUC of the ROC curve, one of the performance evaluation metrics in machine learning: 0.936, 0.965, and 0.970 for each mass point respectively.

This indicates that m_{x_1} achieves better separation from the background for high-signal points.

BDT parameter information and ROC

NTree, maxDepth = (4000, 6) for all mass point case

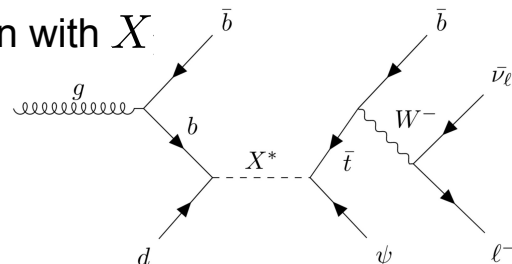
AUC of ROC : described in the right-side table



m_{x_1}	ROC AUC
1.0 TeV	0.936
1.5 TeV	0.965
2.0 TeV	0.970

Results; Comparison with Monotop channel^[4]

- Another search with b-associated monotop channel provides a complementary probe to the monojet channel through **top-quark** production with X

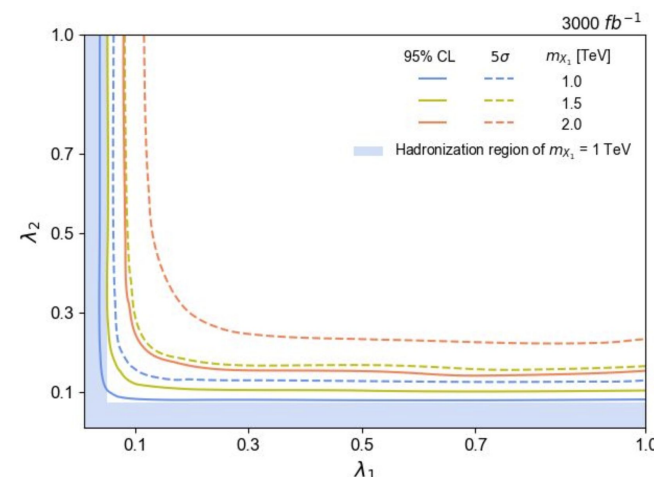
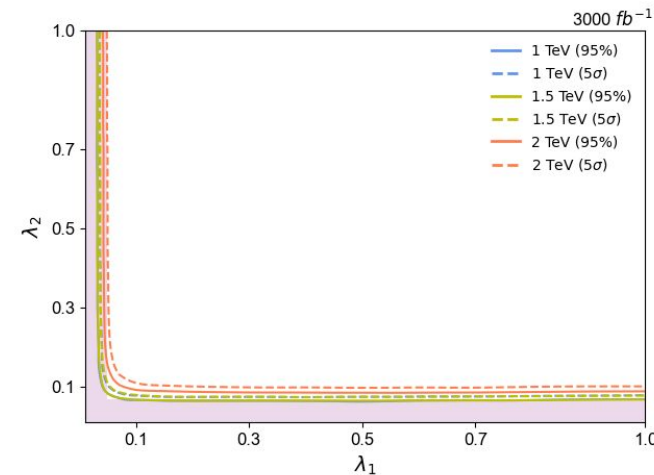


- Exclusion region (95% CL), **HL-LHC (3000 fb^{-1})**

monojet	m_{X_1} [TeV]		
	1.0	1.5	2.0
λ_1	0.03	0.03	0.04
λ_2	0.06	0.06	0.09

monotop	m_{X_1} [TeV]		
	1.0	1.5	2.0
λ_1	0.04	0.05	0.08
λ_2	0.08	0.11	0.15

- Cross-section** for b-associated monojet channel enhanced by a **factor of five than the monotop channel**
⇒ Higher statistics extend the exclusion limit



[4] Amandeep Kaur Kalsi and others, 'Probing Bottom-Associated Production of a TeV Scale Scalar Decaying to a Top Quark and Dark Matter at the LHC', Journal of High Energy Physics, 2024.9 (2024), doi:10.1007/JHEP09(2024)203.